PAPER • OPEN ACCESS

Evaluation of the WRF model for simulating surface winds and the diurnal cycle of wind speed for the small island state of Fiji

To cite this article: K K Dayal *et al* 2020 *J. Phys.: Conf. Ser.* **1618** 062025

Evaluation of the WRF model for simulating surface winds and the diurnal cycle of wind speed for the small island state of Fiji

K K Dayal[1*], J E Cater[2], M J Kingan[1], G D Bellon[3] and R N Sharma[1]

[1] Department of Mechanical Engineering, University of Auckland, NZ
[2] Department of Engineering Science, University of Auckland, NZ
[3] Department of Physics, University of Auckland, NZ

Email: kday202@aucklanduni.ac.nz

Abstract. Evaluation of the performance of the WRF model is carried out for simulating the surface winds and the diurnal cycle of wind speed for the small island developing state of Fiji at a 1.33 km by 1.33 km grid resolution using 1deg gridded data from NCEP-FNL. Simulations are performed for an austral summer (January 2017) and an austral winter (July 2017) month using the dynamical downscaling and the two-way nested approach. A set of physics parameterization schemes together with topo_wind = 1, 2 and ysu_topdown_pblmix = 1 physics settings associated with YSU PBL scheme are used to correct the surface winds and the diurnal cycle of wind speed. The results reveal that the WRF model is able to capture the surface winds and the diurnal cycle of wind speed on the windward side. Surface winds on the leeward side and the outer islands, show positive bias especially at nighttime for January and at both the day and night time for July. The statistical evaluation of all stations for January (July) showed a bias of 1.16 m/s (1.89 m/s), RMSE of 2.40 m/s (3.14 m/s), STDE of 1.88 m/s (2.08 m/s) and diurnal cycle correlation of 0.74 (0.68) using topo_wind = 2 and ysu_topdown_pblmix = 1.

Keywords: WRF, surface winds, diurnal cycle, Fiji.

1. Introduction

Wind resource assessment is an integral part of determining the potential of wind energy for electrical power generation [1, 2]. When assessing the wind resource on a national basis, the application of mesoscale models is most suitable in comparison with other available methods [3]. However, such an assessment becomes a challenging task when applying mesoscale models like the WRF model at high spatial resolution, given the high computational cost [4]. For a small island state surrounded by vast expanses of the ocean, the weather and climate are mainly influenced by the land-sea interaction, which can create further modelling challenges. In addition, if such an island experiences wind flow from a predominant direction, the climate on either (leeward or windward) side of the islands could vary significantly, with the leeward (windward) side being much dryer (wetter). Moreover, additional difficulties may arise in the prediction of surface winds if the mesoscale model is unable to accurately capture significant differences in topography between the two sides [5].

Two methods are available in the WRF model for correcting surface winds: firstly, topographic correction to represent extra drag from sub-grid topography and enhanced flow at hilltops based on the concept of a momentum sink term (c_t) and makes use of the standard deviation of the subgrid-scale orography (σ_{sso}) as well as the Laplacian of the topographic field ($\Delta^2 h$) [6]. The momentum sink term (c_t) stands for the correction of topography and modulates the surface drag associated with vegetation in the momentum-conservation equation:

$$\frac{\partial u}{\partial t} = \cdots - c_t \frac{u_*^2}{\Delta z} \frac{u}{V} \qquad (1)$$

Where u stands for the zonal wind component at the first model level, V is the wind speed also at the first model level, u_* is the frictional velocity that comes from the surface-layer scheme, and Δz is the thickness of the first model layer. A similar modification is also used for the meridional wind equation. The momentum sink term is defined using thresholds, so c_t is larger over valleys and in areas with large σ_{sso}, and tends to zero when $\Delta^2 h < -20\,m$, assuming no drag over hills and mountaintops. It was found that this correction was successful in reducing the large biases found in surface wind speed over-estimation in flat and valley regions [6].

Secondly, a simpler terrain variance-related correction, which determines the subgrid terrain variance and makes the surface drag, or roughness, used in the model, dependent on it; also included is additional consideration for stability and wind speed [7].

The WRF model has been used to study various atmospheric parameters, which includes temperature and precipitation [8], relative humidity [9], low-level jets [10], wind speed and wind direction [11], extreme winds [12] and fire weather index [13] amongst many others over larger landmasses. The WRF model evaluation studies include evaluating winds and the vertical wind shear at a coastal site over western Denmark [14], performance evaluation for assessing wind resource in Greece [15], ability to reproduce surface wind direction over complex terrain in the Iberian Peninsula [16], configuration and evaluation for the study of the Hawaiian regional climate [17], model resolution required climatological downscaling over complex terrain along the Eastern Mediterranean [8], and wind simulation and wind energy estimates for Portugal [18]. Typically, for these studies low biases are found between the observed wind speeds and the simulated wind speeds. It was also found that the WRF model has a tendency to overestimate the low wind speeds and underestimate the higher wind speeds.

To date, most downscaling studies for numerous atmospheric parameters have been conducted in the mid-latitude regions of the Northern Hemisphere and relatively few have examined semi-arid or tropical locations.

In this study, we consider Fiji, which is a small island developing state (SIDS) located in the tropical southwest pacific, with a poorly exploited wind resource and limited knowledge of the wind energy potential. Fiji falls in the trade winds zone with a predominant southeast wind direction and has a tropical marine climate with austral summer (wet season, Nov -Apr) and austral winter (dry season, May - Oct). For a semi-arid tropical country, one of the most important wind resource parameters of the surface winds is the diurnal cycle of the wind speed, which is representative of the land and sea breeze along with the dominant seasonal winds. The WRF numerical weather prediction model can be used to create knowledge about mesoscale surface winds and the diurnal cycle of the wind speed for the SIDS of Fiji.

This study aims to apply the dynamical downscaling method to the semi-arid tropical location of the southwest pacific region to evaluate the capability of the WRF model in simulating the surface winds (10 m) and the diurnal cycle of wind speeds, for the SIDS of Fiji, for an austral summer and an austral winter month.

2. Methodology

2.1 Study area and measured wind data

Figure 1 shows the study area (d03), which is the SIDS of Fiji between the latitudes of 15.5 °S to 19.5 °S and longitudes of 177 °E to 179 °W. Fiji has more than 332 islands with a total land area of 18,333-km^2 spread over a sea surface area of 1.3 million km^2. One-third (110) of these islands are inhabited. Around 87 % of the total land area is taken up by the two largest islands of Viti Levu (10,400 km^2) and Vanua Levu (5,540 km^2). The islands are of volcanic origin, mountainous and with maximum peaks of 1300 m. This study focus on the two larger islands, and other islands that fall within d03.

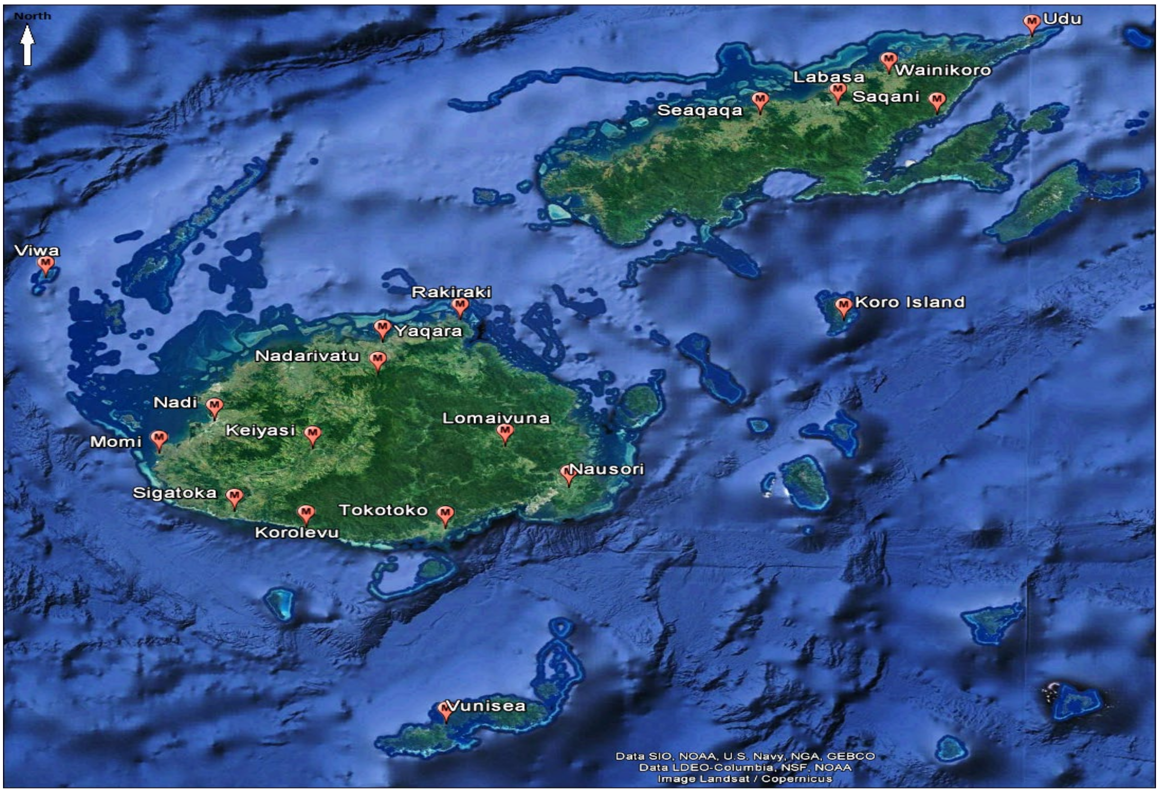

Figure 1. Map of the study area (d03) including locations of the 19 AWS (Source: Google Earth).

Table 1. Details and position of the AWSs

Station name	Latitude (° S)	Longitude (° E)	Elevation (m a.s.l.)	Elevation in WRF (m a.s.l.)
Keiyasi	-17.8795	177.7552	89.8	79.7
Koro Island	-17.3450	179.4184	108.8	174.7
Korolevu	-18.2129	177.7304	25.7	39.8
Labasa	-16.4333	179.4000	8.5	4.5
Lomaivuna	-17.8714	178.3601	122.1	125.2
Momi	-17.8952	177.2668	43.8	24.5
Nadarivatu	-17.5676	177.9632	824.1	701
Nadi	-17.7599	177.4448	20.7	11.7
Nausori	-18.0464	178.5591	5.7	5.2
Rakiraki	-17.3404	178.2214	8.1	0.7
Saqani	-16.4749	179.7089	30.0	39.1
Seaqaqa	-16.4758	179.1578	101.8	109.4
Sigatoka	-18.1422	177.5039	6.7	37.8
Tokotoko	-18.2186	178.1700	4.9	5.6
Udu	-16.1411	-179.9947	43.7	0.9
Viwa	-17.1494	176.9117	2.0	0.7
Vunisea	-19.0469	178.1654	31.9	35.9
Wainikoro	-16.3044	179.5586	15.1	28.8
Yaqara	-17.4330	177.9774	20.0	8.8

Measured wind data at 10 m elevation is available from 19 Automatic Weather Stations (AWSs) located around Fiji for the months of January and July of 2017. The locations of the AWSs can be seen in Figure 1, where eleven stations are located on Viti Levu, five on Vanua Levu and three on the outer islands. The AWSs located on the windward side of the larger islands are Korolevu, Lomaivuna, Nausori, Saqani, Tokotoko and Udu. The AWSs located on the leeward side of the larger islands are Keiyasi, Labasa, Momi, Nadarivatu, Nadi, Rakiraki, Seaqaqa, Sigatoka, Wainikoro and Yaqara. The AWSs located on the outer islands are Koro Island, Viwa and Vunisea. Table 1 shows the summary of the characteristics of the AWSs from which the wind observations are retrieved. The elevation is given in meters above sea level (m a.s.l.). Also, included are the model terrain heights of the closest grid point to each of these AWS locations.

2.2 Model and simulation setup

The study used the Advanced Research WRF (ARW) [19, 20] atmospheric mesoscale model version 3.9.1. The dynamical downscaling method was used for running the simulations using the WRF model. This method uses the output from General Circulation Models (GCM) as input initial and boundary conditions to drive a regional numerical model to simulate atmospheric parameters at a high spatial resolution via direct nesting, taking into account the local conditions [21, 22].

The initial and boundary conditions for Fiji were obtained from 6-hourly NCEP-FNL (Final) Operational Global Analysis data at 1° × 1° grid resolution [23]. The static fields for topography was obtained from USGS GMTED2010, land-water masks, land use/land cover classification and albedo, etc., were obtained and interpolated from the 21-class MODIS and MODIS FPAR, all these made available from the National Center for Atmospheric Research (NCAR) database, at a resolution of 30-arc-seconds. Time-varying SSTs were supplied to the model from NCEP-NOAA at 0.083° × 0.083° grid resolution.

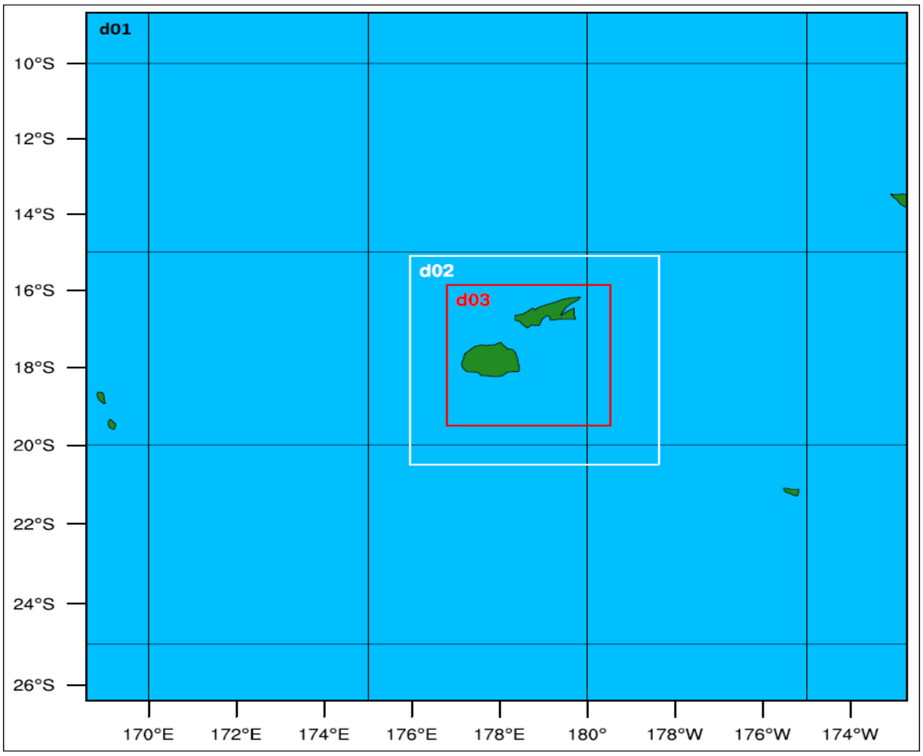

Figure 2. WRF domain d01, d02 and d03 with 20 km, 4 km and 1.33 km resolutions respectively.

The NCEP-FNL data were downscaled by the WRF model using three domains as illustrated in Figure 2. The outermost domain hereafter referred to as d01, second d02 and the innermost as d03. The grid size for the domains is reduced by a factor of 5 from 20 km in d01 to 4 km in d02 and by a factor of 3 from 4 km in d02 to 1.33 km in d01. The 20 km – 4 km – 1.33 km nested grids have been used because the islands are smaller and the topography changes every 100 – 500 m. The standard practice of using a 3:1 or 5:1 parent-grid ratio has been followed [19, 20]. A two-way nesting approach is applied, whereby the flow of information goes from the coarser domains to the finer domains, with feedback from the inner domains. The averaged values over the grid points from the inner domain are sent back to the parent domains to overwrite values at corresponding grid points. The two-way nesting approach was used so that the coarser grid results can be improved using the higher-resolution grid results of the inner domain in case of resource mapping for the outer domains. As in this way, the results from a better resolved topography of the finest grid is used to overwrite the results of the outer grids improving its results. The centre of d01 is at a latitude of 17.73 °S and longitude of 177.94 °E, which corresponds to the centre of Viti Levu. The Mercator projection is used as recommended for lower latitudes [19, 20]. The areas covered by each of the domains are: $\mathrm{d01} = 2000\ \mathrm{km} \times 2000\ \mathrm{km}$, $\mathrm{d02} = 604\ \mathrm{km} \times 604\ \mathrm{km}$ and $\mathrm{d03} = 399\ \mathrm{km}\ 399\ \mathrm{km}$ at horizontal resolutions of $20\ \mathrm{km} \times 20\ \mathrm{km}$, $4\ \mathrm{km} \times 4\ \mathrm{km}$ and $1.33\ \mathrm{km} \times 1.33\ \mathrm{km}$ respectively. The vertical structure of the three domains consist of 30 terrain-following vertical coordinates, including eight levels below 1 km, as the interest is in the lower part of the atmosphere closer to surface. This was done to balance between the computational cost and the computational time. A timestep of 10 seconds is used in d03 to ensure numerical stability as recommended [19, 20].

The tropical suite of the physics parameterization scheme [19, 20] was used, which included the RRTMG longwave and shortwave radiation schemes [24], the WRF single-moment 6-class microphysics scheme [25], the New Tiedtke cumulus parameterization scheme [26], the Noah land surface model [27], the MM5 Similarity scheme [28] for the surface layer, and the Yonsei University Planetary Boundary Layer scheme [29]. These are well-tested physics parameterization schemes in WRF applications in the tropics [19, 20].

The monthly simulations were performed on the New Zealand eScience Infrastructure (NeSI) High Performance Computer – Mahuika for a simulation time of 3 days for the 34 day monthly simulations. The first 6.35 hours of simulation, which is equivalent to 3 days, are considered to be spin-up time for the simulations and are excluded from the analysis. Even though a period of one year is considered sufficient to capture diurnal and seasonal variations for wind resource assessments [30], in our case one month of either seasons is considered. This is done to evaluate if the model is able to simulate the surface winds and the diurnal cycle of wind speeds before longer simulations in the order of few years to 10 years can be simulated. All the results discussed in the paper are 1-hourly values retrieved from the inner most domain (d03) at 10 meter height above the ground from the same points as the AWS locations. The grid cell containing the station in the domain is used to achieve this. Table 1 lists the model terrain height for the closest grid point to each of the 19 AWSs.

Additional physics settings were used to correct the surface winds and the diurnal cycle of wind speed for January 2017 against ground-based measurements from AWSs. These included topo_wind = 0/1/2, ysu_topdown_pblmix = 1, Varsso = 30 arc seconds, changing the surface layer scheme from MM5 (sf_sfclay_physics = 91) to Modified MM5 (sf_sfclay_physics = 1) and doubling surface roughness for the dominant land use categories. The surface roughness was doubled in an attempt to see if there is any improvement in the model mean wind speed and the diurnal cycle of wind speed. Doubling the surface roughness made the surface winds almost constant throughout the entire day with limited diurnal variation. These were done to see what effect each of the settings had on the surface winds and the diurnal cycle of wind speed and if these could improve the model results. Then, the best setting was used to simulate the surface winds for July 2017.

2.3 Model Evaluation

The 10 m surface winds simulated by the model were validated using measurements from the 19 AWSs. The three statistical parameters used for evaluation are according to [31]. The Root Mean Squared Error

(RMSE) was used, which represents the deviation between the simulated M_i and respective observed O_i data in the same place and time instant, and N is the total number of data points:

$$RMSE = \left[\frac{1}{N}\sum_{i=1}^{N}(M_i - O_i)^2\right]^{\frac{1}{2}} \qquad (2)$$

The Bias was used for the evaluation of the data tendency. A positive (negative) bias means the simulations overestimate (underestimate) the measured values:

$$Bias = \frac{1}{N}\sum_{i=1}^{N}(M_i - O_i) \qquad (3)$$

The Standard Deviation Error (STDE) was used to evaluate the dispersion of the error between observed and simulated data:

$$STDE = \left[\frac{1}{N}\sum_{i=1}^{N}(M_i - O_i)^2 - \frac{1}{N}(M_i - O_i)^2\right]^{\frac{1}{2}} \qquad (4)$$

Priority is given to STDE, and this assumption comes from the fact that, even if a simulation has a high RMSE or Bias, if the STDE is low it means that the error is somewhat constant and can be seen as a kind of offset and the simulation physics is correct. If a simulation has a high STDE, the error is random and the simulation has low physical meaning, even if it has a relatively low RMSE or Bias [31, 32].

The Pearson correlation coefficient was used to evaluate the diurnal cycle. The Pearson correlation coefficient is a statistical measure that calculates the strength of the relationship between the relative movement of two variables; in our case, the simulated and measured monthly averaged diurnal values.

3. Results

Table 2 presents the evaluation of the surface winds and the diurnal cycle of wind speed for the different physics settings. The best model configuration tested was with the topo_wind = 2 and ysu_topdown_pblmix = 1 physics settings for d03 as it has the lowest STDE and Bias for the surface winds and the highest diurnal cycle correlation of wind speed for January 2017.

Table 2. Evaluation of surface winds and the diurnal cycle for different physics settings

Physics settings -	Month	Observed Mean (m/s)	WRF Mean (m/s)	Bias (m/s)	RMSE (m/s)	STDE (m/s)	Diurnal Cycle Correlation (%)
topo_wind = 1 ysu_topdown_pblmix = 1	Jan	2.23	3.47	1.24	2.40	1.88	0.64
topo_wind = 2 ysu_topdown_pblmix = 1	**Jan**	**2.23**	**3.39**	**1.16**	**2.40**	**1.88**	**0.74**
topo_wind = 1 ysu_topdown_pblmix = 1 Varrso = 30 s	Jan	2.23	3.45	1.22	2.38	1.89	0.69
topo_wind = 2 ysu_topdown_pblmix = 1 Modified MM5	Jan	2.23	3.49	1.26	2.38	1.88	0.67
Topo_wind = 0 Major roughness categories doubled	Jan	2.23	3.50	1.27	2.40	1.90	0.66
topo_wind = 2 ysu_topdown_pblmix = 1	**Jul**	**3.37**	**5.26**	**1.89**	**3.14**	**2.08**	**0.68**

The WRF simulated average wind speed over all the locations in January (July) is 3.39 m/s (5.26 m/s), with a bias of 1.16 m/s (1.89 m/s), RMSE of 2.40 m/s (3.14 m/s), STDE of 1.88 m/s (2.08 m/s) and diurnal cycle correlation of 0.74 (0.68). The observed and the model dominant wind direction is southeasterly. Since the STDE for both months studied is ≤ 2 m/s, this indicates that the model physics is correct [30, 31]. The mean value across all the AWSs is used in Table 2 to evaluate the overall model performance for the 19 AWSs and the 5 different scenarios for evaluating the surface winds and the diurnal cycle wind speed.

Tables 3 and 4 present the individual statistical evaluation of surface winds and the diurnal cycle of wind speed respectively, for each AWS for January and July of 2017. AWSs located on the windward side and in relatively flat terrain have a lower bias and higher diurnal cycle correlation. AWSs located on the leeward side, outer islands and in complex terrain have a higher bias and a lower diurnal cycle correlation. This indicates that the terrain on the leeward side is not adequately resolved in the model.

Table 3. Evaluation of surface winds and the diurnal cycle of wind speed for Fiji for Jan 2017

Station	Measured Mean (m/s)	WRF Mean (m/s)	Bias (m/s)	RMSE (m/s)	STDE (m/s)	Diurnal Cycle Correlation %
Keiyasi	1.00	3.60	2.62	3.38	2.10	0.91
Koro Island	2.62	3.50	0.87	2.08	1.89	0.59
Korolevu	3.18	4.22	1.04	2.57	2.25	0.89
Labasa	1.21	3.25	2.04	2.63	1.66	0.86
Lomaivuna	1.69	1.97	0.27	1.29	1.26	0.95
Momi	3.56	3.96	0.40	2.21	2.10	0.94
Nadarivatu	1.67	3.90	2.22	2.99	2.00	-0.33
Nadi	2.73	3.66	0.93	2.70	2.40	0.93
Nausori	1.40	1.51	0.11	1.46	1.46	0.95
Rakiraki	4.08	3.34	-0.73	2.31	2.20	0.74
Saqani	1.65	3.43	1.78	2.34	1.53	0.45
Seaqaqa	1.17	3.41	2.24	2.82	1.72	0.95
Sigatoka	1.77	4.24	2.47	3.26	2.12	0.86
Tokotoko	2.14	1.83	-0.31	1.17	1.13	0.97
Udu	3.55	3.59	0.03	1.83	1.83	0.40
Viwa	2.42	4.50	2.08	3.01	2.18	0.46
Vunisea	2.30	3.70	1.40	2.98	2.50	0.84
Wainikoro	1.00	3.10	2.09	2.55	1.46	0.93
Yaqara	3.26	3.81	0.55	2.08	2.01	0.75
Average	2.23	3.40	1.16	2.40	1.88	0.74

Figures 3 and 4 present the wind speed diurnal cycles for austral summer (January) and austral winter (July) of 2017, for the windward and the leeward sides of the main islands and the outer islands. Long observational datasets available in the order of 5 – 8 years have similar diurnal cycle patterns for the months of January and July of 2017 used in this study. The WRF model is able to simulate the full diurnal cycle of wind speed on the windward side stations for both January and July. For the leeward side and the outer island stations, the model is able to simulate the daytime wind speed but there is a positive bias in the nighttime for January. For July, the modelled wind speeds for both the outer islands and the leeward side, show poor diurnal cycle predictions, and a positive bias for both the day and the nighttime. The possible reasons for the observed bias include the limitations of the model in terms of the errors associated with the coarse resolution input data used as initial and boundary conditions, resolution of the domain, terrain and vegetation characteristics and the complexity of the terrain and its representation in the model. The choice of physical schemes can also contribute to errors in the model, as these schemes are based on assumptions, and these assumptions may fail, or give an inadequate response to certain synoptic forcing, limiting their application [33], for instance the PBL scheme works better during the day than at night [34].

Table 4. Evaluation of surface winds and the diurnal cycle of wind speed for Fiji for Jul 2017

Station	Measured Mean (m/s)	WRF Mean (m/s)	Bias (m/s)	RMSE (m/s)	STDE (m/s)	Diurnal Cycle Correlation %
Keiyasi	1.10	5.63	4.53	4.99	2.11	0.46
Koro Island	4.31	6.17	1.86	2.56	1.77	0.50
Korolevu	3.24	6.14	2.90	3.63	2.17	0.83
Labasa	2.20	5.24	3.05	3.84	2.34	0.83
Lomaivuna	1.97	2.24	0.27	1.22	1.19	0.91
Momi	4.68	5.84	1.16	2.61	2.34	0.87
Nadarivatu	3.29	5.98	2.70	3.28	1.87	0.45
Nadi	3.31	5.49	2.18	3.28	2.45	0.81
Nausori	1.55	1.61	0.06	1.34	1.34	0.98
Rakiraki	6.96	5.29	-1.67	2.93	2.41	0.84
Saqani	2.83	5.50	2.67	3.31	1.95	0.43
Seaqaqa	1.58	5.44	3.86	4.48	2.28	0.65
Sigatoka	1.96	6.18	4.23	4.76	2.19	0.83
Tokotoko	2.47	2.21	-0.25	1.38	1.36	0.90
Udu	7.09	6.34	-0.75	2.59	2.48	0.71
Viwa	4.85	6.08	1.23	3.37	3.14	0.83
Vunisea	3.40	7.16	3.76	4.35	2.18	-0.12
Wainikoro	2.27	5.22	2.95	3.57	2.01	0.87
Yaqara	4.99	6.12	1.12	2.19	1.88	0.41
Average	3.37	5.26	1.89	3.14	2.08	0.68

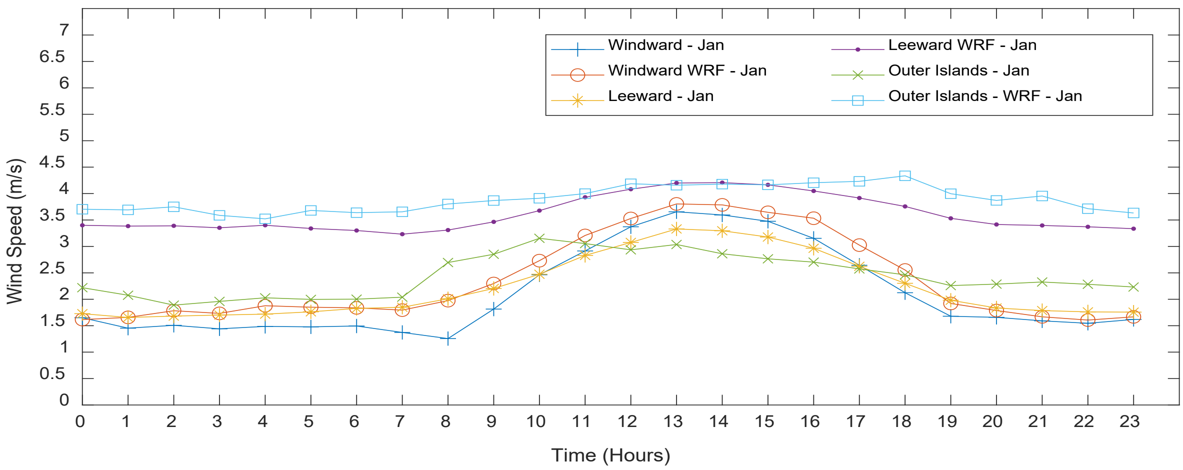

Figure 3. Wind speed diurnal cycle for different locations in Fiji for Jan 2017.

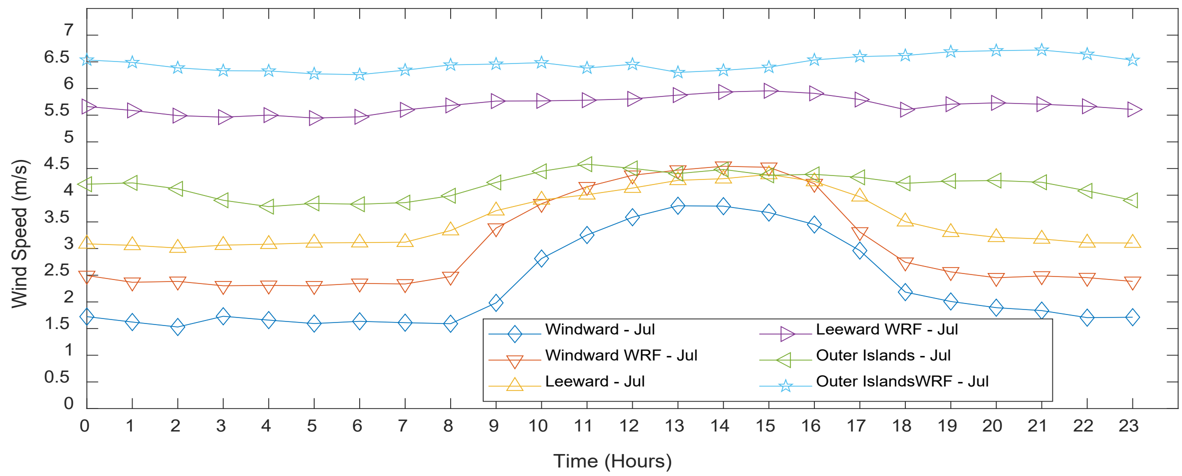

Figure 4. Wind speed diurnal cycle for different locations in Fiji for Jul 2017.

Figures 5 and 6 show the average 10 m wind speeds for the austral summer (January) and austral winter (July) of 2017. The winds in austral summer (austral winter) are lower (higher) in the order of 1 – 4.5 m/s (1 – 8 m/s) over land areas. Higher wind speeds are observed in the windward side and western and eastern near-offshore areas of the larger islands, and in the channel (Bligh Waters) between the two larger islands.

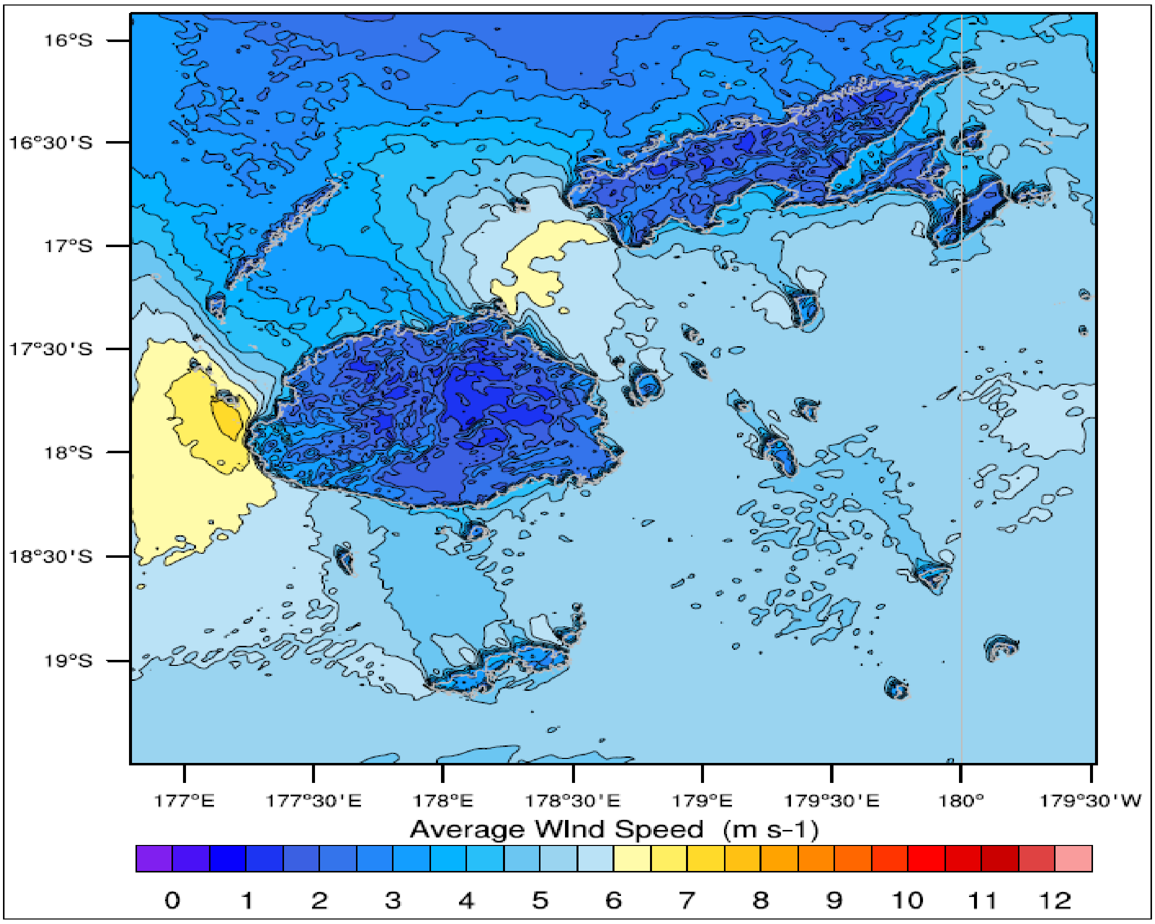

Figure 5. Average 10 m elevation wind speed of Fiji for a month of austral summer (Jan 2017).

Wakes generated by the islands topography are observed from islands during summer and mostly one island during winter. This is due to the presence of higher altitude topography on Viti Levu and the southeast trade winds, which are more persistent during austral winter. During austral summer, the trade winds are weaker and the wind climate is dominated by synoptic systems.

The results of the simulations are useful for the wind industry as it presents the first validated mesoscale wind-resource maps for either months of the two different seasons for the SIDS of Fiji. The spatial distribution of the surface wind speeds indicates areas of lower, moderate and higher winds probable for potential wind resource sites, which can be further investigated once simulations in the order of 5 – 10 years are performed. It also shows that the SIDS of Fiji has areas of moderate and higher winds, which can be utilized for power generation using wind turbines.

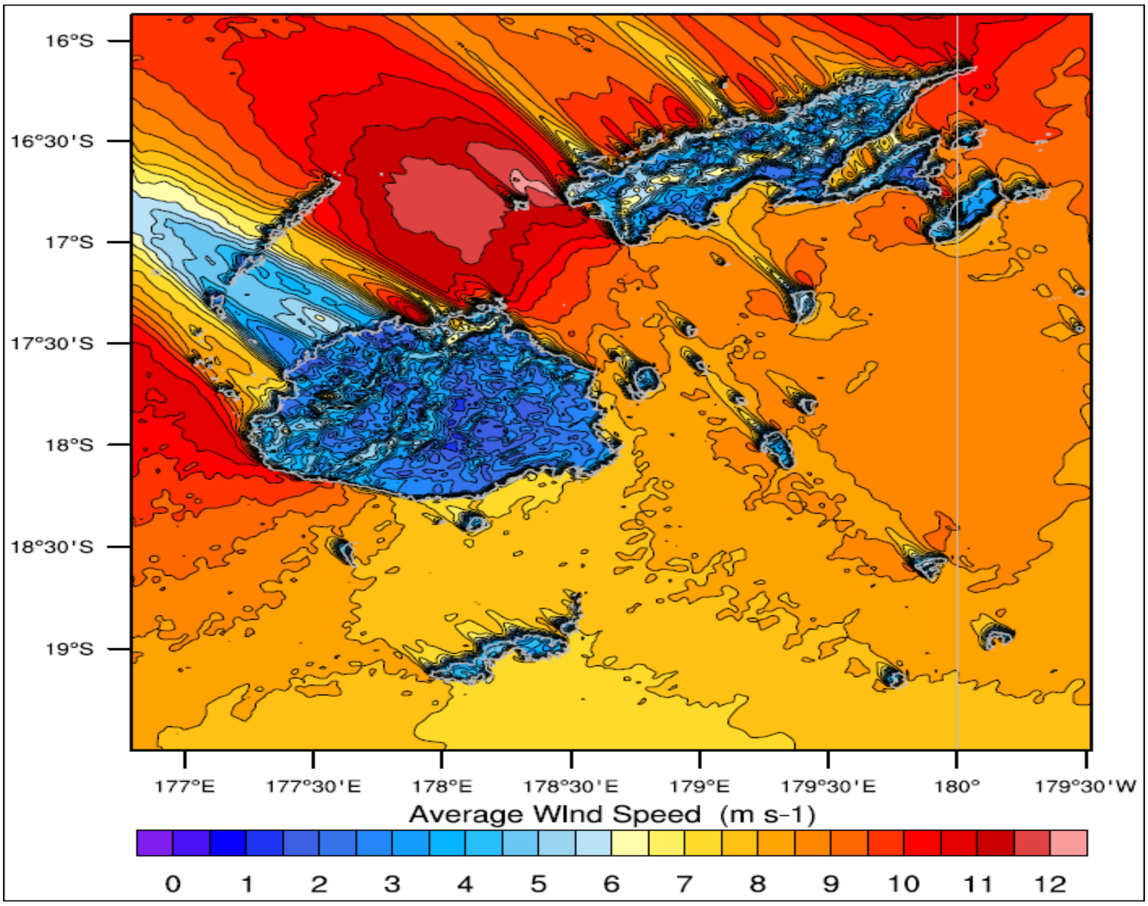

Figure 6. Average 10 m elevation wind speed of Fiji for a month of austral winter (Jul 2017).

For the purpose of long term (i.e. in the order of 5 – 10 years) mesoscale wind resource assessment for a SIDS like Fiji, it is fundamental to predict correct surface winds and especially the diurnal cycle of wind speed. The diurnal cycle is a representation of the land and the sea breeze interaction of the tropical island location with the vast ocean component surrounding the islands. Once long term mesoscale wind-resource results are available, it can assist the SIDS of Fiji to identify potential wind resource sites, which can be utilized for future wind farm developments to assist the country towards its renewable electrical power generation.

For a further study, a grid sensitivity study is currently underway to identify an appropriate model grid size that is able to capture the surface winds and especially the diurnal cycle of wind speed not only on the windward side but also on the leeward side. The AWSs on the leeward side are mostly located in complex terrain, thus, it would be interesting to see the effect of reduced grid sizes in the order of

1 km × 1 km and 0.8 km × 0.8 km resolutions on the surface winds and the diurnal cycle of wind speed over the SIDS of Fiji.

4. Conclusions

An evaluation of the WRF model to simulate the surface winds and the diurnal cycle of wind speed has been carried out for the SIDS of Fiji at a high spatial resolution of 1.33 km by 1.33 km. The NCEP-FNL 1deg atmospheric input data was used to drive the WRF model simulations via two-way nested approach for an austral summer (January) and an austral winter (July) month of 2017. A set of physics parameterization schemes were tested with additional physics settings associated with the YSU PBL scheme to correct the surface winds and the diurnal cycle of wind speed against measurements from AWSs. The results showed that the WRF model is able to accurately capture the surface winds and the diurnal cycle of wind speed on the windward side. Surface winds on the leeward side and the outer islands, show positive bias especially at night for January and both the day and night for July, despite adjusting some of the physics settings, showing the limitations of the model. The statistical evaluation of all the stations for January (July) showed a bias of 1.16 m/s (1.89 m/s), RMSE of 2.40 m/s (3.14 m/s), STDE of 1.88 m/s (2.08 m/s) and diurnal cycle correlation of 0.74 (0.68) using topo_wind = 2 and ysu_topdown_pblmix = 1.

A grid sensitivity study is underway to further investigate if reducing the grid size of the model simulation domain can better capture the surface winds and especially the diurnal cycle of wind speed for not only the windward side but also the leeward side AWS locations.

Acknowledgement

This study is part of a PhD research project, for which the lead author is the recipient of scholarship funding from the New Zealand Ministry of Foreign Affairs and Trade (NZMFAT). The authors gratefully acknowledges the Fiji Meteorological Services for providing the ground-based wind data measurements from AWSs in Fiji and the New Zealand eScience Infrastructure (NeSI) for use of the high-performance computing facilities in this research.

5. References

[1] Manwell J F, McGowan J G and Rogers A L 2009 *Wind Energy Explained: Theory, Design and Application* (Chichester: John Wiley & Sons)
[2] Carvalho D, Rocha A, Gómez-Gesteira M and Silva Santos C 2014 *Applied Energy* **117** 116-126
[3] Foley A M, Leahy P G, Marvuglia A and McKeogh E J 2012 *Renewable Energy* **37(1)** 1-8
[4] Prein A F et al 2015 *Reviews of Geophysics* **53(2)** 323-361
[5] Lehner M and Rotach M W 2018 *Atmosphere* **9(7)** 276
[6] Jimenez P A and Dudhia J 2012 *Journal of Applied Meteorology and Climatology* **51** 300-316
[7] Mass and Ovens 2011 *24th Conf. on Weather and Forecasting/20th Conf. on NWP* 9B.6
[8] El-Samra R, Bou-Zeid E and El-Fadel M 2018 *Atmospheric Research* **203** 68-82
[9] Kryza M, Walaszek K, Ojrzynska H, Szymanowski M, Werner M and Dore A J 2017 *Pure and Applied Geophysics* **174** 511-526
[10] Storm B, Dudhia J, Basu S, Swift A and Giammanco 2009 *Wind Energy* **12(1)** 81-90
[11] De Meij A, Vinuesa J-F, Maupas V, Waddle J, Price I, Yaseen B and Ismail A 2016 *Renewable and Sustainable Energy Reviews* **56** 551-562
[12] Larsén X G, Badger J, Hahmann A N, and Mortensen N G 2013 *Wind Energy* **16** 1167-1182
[13] Simpson C C, Pearce H G, Sturman A P and Zawar-Reza P 2013 *International Journal of Wildland Fire* **23** 34-45
[14] Caroline D, Andrea N H, Alfred P and Gregor G 2012 *Wind Energy* **17** 39-55
[15] Giannaros T M, Melas D and Ziomas I 2017 *Renewable Energy* **102** 190-198
[16] Jimenez P A and Dudhia J 2013 *Journal of Applied Meteorology and Climatology* **52** 1610-1617
[17] Zhang C, Wang Y, Lauer A and Hamilton K 2012 *Monthly Weather Review* **140(10)** 3259-3277
[18] Carvalho D, Rocha A, Gómez-Gesteira M and Santos C S 2014 *Applied Energy* **117** 116-126

[19] Skamarock W C, Klemp J B, Dudhia J, Gill D O, Barker D M, Duda M G, Huang X Y, Wand W and Powers J G 2008 Technical Report NCAR/TN-475+STR
[20] Wang W et al 2018 ARW User Guide V3.9
[21] Hewitson B C and Crane R G 1996 *Climate Research* **7** 85-95
[22] Hong S-Y & Kanamitsu M 2014 *Asia-Pacific Journal of Atmospheric Sciences* **50(1)** 83-104
[23] NCEP/NWS/NOAA/U.S. Depart. of Com. 2015 Research Data Archive at NCAR CIS Laboratory
[24] Iacono M J, Delamere J S, Mlawer E J, Shephard M W, Clough S A and Collins W D 2008 *Journal of Geophysical Research* **113** D13103
[25] Hong S-Y and Lim J-O J 2006 *Journal of Korean Meteorological Society* **42** 129–151
[26] Zhang C and Wang Y 2017 *Journal of Climate* **30** 5923-5941
[27] Tewari M et al 2004 *20th Conf. on Weather analysis and Forecasting/16th Conf. on NWP* 11-15
[28] Beljaars A C M 1994 *Quarterly Journal of the Royal Meteorological Society* **121** 255-270
[29] Hong S-Y, Noh Y and Dudhia J 2006 *Monthly Weather Review* **134(9)** 2318–2341
[30] Al-Yahyai S, Charabi Y and Gastli A 2010 *Renewable and Sustainable Energy Reviews* **14** 3192-3198
[31] Carvalho D, Rocha A, Gómez-Gesteira M and Santos C 2012 *Environmental Modelling & Software* **33** 23-34
[32] Emery C, Tai E and Yarwood G 2001 *Environmental Final Report* **31984-11** 235
[33] Awan N K, Gobiet A and Truhetz H 2011 *Journal of Climate* **24** 3107-3123
[34] Holtslag A A M et at 2013 *Bulletin of American Meteorological Society* **94(11)** 1671-1706